

1 Reply to Reviewer's comments

2 *General Comments*

3 *Although the figure quality has improved, the language still needs to be
4 improved substantially before final publication.*

5
6 Response: Appreciate your further comments. Figures and sentences have been
7 updated again and wish it would help.

8
9 *Detailed Comments:*

10 *1. Further model detail needs to be provided in the manuscript itself. The reader
11 shouldn't have to refer to the author's responses for details on the boundary layer
12 height assumed.*

13
14 Response: Thanks for the advice. The sentence was added in the end of section 2.3.1.
15 The boundary layer height was set as constant as 1000 m in the model due to the lack
16 in measurements. This was similar to model setups in Lu et al (2013) and field
17 measurement results in Guo et al (2016).

18
19 *2. The authors suggest that they have run the model for different spin up times and
20 report a difference within 10%, but no detail on the different spin up times tested is
21 provided!*

22
23 Response: Appreciate the suggestion. There was also one more sentence in section
24 2.3.1 in the latest version of manuscript. Different scenarios with 1 day, 2 days and 3
25 days spin-up time have been tried while the differences were within 10%.

26
27 *3. I still think it is important to include a time-series of measured, calculated and
28 modelled reactivity somewhere in the manuscript. If there is missing data for the
29 Beijing campaign, just leave gaps in the time-series rather than interpolate. The
30 pie-charts generated from the campaign averages hide a lot of detail - e.g. diurnal
31 variation and day to day variability.*

32
33 Response: Thanks for the suggestion. The missing data really caused a lot of problems
34 for the data evaluation. However, we follow the suggestion from the reviewers and
35 revised Fig 5a and Fig 5b as in the latest version. However, this suggestion was an
36 important one, especially for the last sentence: the averages hide a lot of details.

37
38 *4. Paris is still not included in figure 10b (and has now been removed from fig. 10a,
39 but is still discussed in section 4.1).*

40
41 Response: Thanks for the suggestion. The sentence including Paris information were
42 deleted in the latest version. Sorry for the careless mistake. The figures remained as in
43 the last version.

44
45 *5. Mention that the NOAA 2005 dataset was from Beijing in the manuscript. Include a*
46 *comment on the sensitivity of OPE to the species chosen to represent the missing*
47 *reactivity in section 4.4.*

48
49 Response: Appreciate the suggestion. For the first one, we add “Beijing” in the first
50 same sentence referring to NOAA measurements in 2005. For the second one, we
51 rephrased the sentence in section 4.4 as follows:
52 When the four branched-alkenes were included in the OPE calculation, the OPE
53 results would be 4% higher than the OPE constrained by calculated reactivity, but still
54 far from the OPE constrained by measured reactivity.
55 This suggestion was very good, which connected both the results in section 4.2 and
56 section 4.4.

57
58
59
60
61
62
63
64
65
66
67
68
69
70
71
72

73 **How does the OH reactivity affect the ozone production efficiency:**

74 **case studies in Beijing and Heshan, China**

75

76 Yudong Yang¹, Min Shao^{1,*}, Stephan. Keßel², Yue Li¹, Keding Lu¹, Sihua Lu¹,
77 Jonathan Williams², Yuanhang Zhang¹, Liming Zeng¹, Anke C. Nölscher^{2,#}, Yusheng Wu¹,
78 Xuemei Wang³, Junyu Zheng⁴,

79

80 ¹ State Joint Key Laboratory of Environmental Simulation and Pollution Control, College of
81 Environmental Science and Engineering, Peking University, Beijing, China

82 ² Department of Atmospheric Chemistry, Max Plank-Institute for Chemistry, Mainz, Germany

83 ³ School of Atmospheric Science, Sun Yat-Sen University, Guangzhou, China

84 ⁴ School of Environmental Science and Engineering, South China University of Technology,
85 China

86 # now at: Division of Geological and Planetary Sciences, California Institute of Technology,
87 Pasadena, USA

88

89 * Corresponding to: Min Shao

90 Email address: mshao@pku.edu.cn

91

92 **Abstract**

93 Total OH reactivity measurements were conducted on the Peking University
94 campus, Beijing in August 2013 and in Heshan, Guangdong Province from October to
95 November 2014. The daily median OH reactivity were $20 \pm 11 \text{ s}^{-1}$ in Beijing and $31 \pm$
96 20 s^{-1} in Heshan respectively. The data in Beijing showed a distinct diurnal pattern
97 with the maxima over 27 s^{-1} in early morning and minima below 16 s^{-1} in the
98 afternoon. The diurnal pattern in Heshan was not as evident as in Beijing. Missing
99 reactivity, defined as the difference between measured and calculated OH reactivity,
100 was observed at both sites, with 21% missing in Beijing and 32% missing in Heshan.
101 Unmeasured primary species, such as branched-alkenes could contribute to missing
102 reactivity in Beijing, especially in morning rush hours. An observation-based model
103 with the RACM-2 (Regional Atmospheric Chemical Mechanism version 2) was used
104 to understand the daytime missing reactivity in Beijing by adding unmeasured
105 oxygenated volatile organic compounds and simulated intermediates of the
106 degradation from primary VOCs. However, the model could not find the convincing

107 explanation for the missing in Heshan, where the ambient air was found to be more
108 aged, and the missing reactivity was presumably attributed to oxidized species, such
109 as unmeasured aldehydes, acids and di-carbonyls. The ozone production efficiency
110 was 21% higher in Beijing and 30% higher in Heshan when the model was
111 constrained by the measured reactivity, compared to the calculations with measured
112 and modeled species included, indicating the importance of quantifying the OH
113 reactivity for better understanding ozone chemistry.

114

115 1. Introduction

116 Studies on total OH reactivity in the atmosphere have been of increasing interest
117 over the last two decades. The instantaneous total OH reactivity, is defined as

$$118 \quad k_{OH} = \sum_i k_{OH+X_i} [X_i] \quad (1-1)$$

119 where X represents a reactive species (CO, NO₂ etc.) and k_{OH+X_i} is the rate
120 coefficient for the reaction between X and OH radicals. Total OH reactivity is an
121 index for evaluating the amounts of reductive pollutants in terms of ambient OH loss
122 and hence their roles in atmospheric oxidation (Williams, 2008; Williams and Brune,
123 2015; Yang et al., 2016). It also provides a constraint for OH budget calculation in
124 both field campaigns and laboratory studies (Stone et al., 2012; Fuchs et al., 2013).

125 Total OH reactivity measuring techniques, e.g., two laser-induced-fluorescence
126 (LIF) based techniques (Calpini, et al., 1999; Kovacs and Brune, 2001) and one
127 proton-transfer-reaction mass spectrometry (PTR-MS) based technique, comparative
128 reactivity method (CRM) (Sinha et al., 2008) were developed in recent years. A brief
129 comparison of these techniques and their interferences were summarized (Yang et al.,
130 2016). By deploying these measuring techniques, total OH reactivity measurements
131 have been intensively conducted in urban and suburban areas. Details of these
132 campaigns were listed in Table 1 and Table 2. Most of the campaigns exhibited
133 similar diel features with higher reactivity in dawn and rush hours of early morning,
134 and lower levels in the afternoon, which could be explained by the change in

135 boundary layer height, emissions and oxidation processes. Anthropogenic volatile
136 organic compounds (VOCs) and inorganics, such as CO and NO_x (NO + NO₂) are
137 major known OH sinks in urban areas.

138 However, a substantial difference between measured and calculated or modelled
139 OH reactivity, termed as the missing reactivity, was revealed in most field campaigns.
140 Compared to the high percentages of missing reactivity in forested areas (Sinha et al.,
141 2010; Nölscher et al., 2012; 2016; Edwards et al., 2013, Williams et al., 2016), most
142 campaigns in urban and suburban areas gave relatively lower percentages of missing
143 reactivity except for the 75% missing reactivity in Paris in MEGAPOLI under the
144 influences of continental air masses (Dolgorouky et al, 2012).

145 Various methods were used in exploring the origins of missing reactivity.
146 Unmeasured primary species are important candidates. Sheehy et al. (2010)
147 discovered a higher percentage of missing reactivity in morning rush hours and found
148 that the unmeasured primary species, including organics with semi and low-volatility,
149 could contribute up to 10% of total reactivity. Direct measurements on reactivity of
150 anthropogenic emission sources were conducted, such as vehicle exhaust and gasoline
151 evaporation. An average of 17.5% missing reactivity was found in vehicle exhaust
152 measurements (Nakashima et al., 2010). For gasoline evaporation, a study showed
153 that if primary emitted branched-chained alkenes were considered, the measured and
154 calculated reactivity then agreed (Wu et al., 2015). Besides primary emitted species,
155 unknown secondary species were not negligible. Yoshino et al. (2006) found a good
156 correlation between missing reactivity and measured oxygenated VOCs (OVOCs) in
157 three seasons except for winter, assuming that the unmeasured OVOCs could be
158 major contributors of missing reactivity, in one case the OVOCs could increase
159 reactivity by over 50% (Lou et al., 2010). The observation-based model (OBM) was
160 widely used to evaluate the measured reactivity (Lee et al., 2010; Lou et al., 2010;
161 Whalley et al., 2016), confirming the important contribution from OVOCs and
162 undetected intermediate compounds.,

163 Ground-level ozone pollution has been of increasing concerns in China. While
164 the ozone concentration exceeds Grade II of China National Ambient Air Quality

165 Standards (2012) (93 ppbV) frequently in summer in Beijing-Tianjin-Hebei area and
166 Pearl River Delta (PRD) region (Wang et al., 2006; Zhang et al., 2008), it appears
167 there is an increasing trend for ozone in Beijing and other area recent years (Zhao et
168 al., 2009; Zhang et al., 2014). Comparing to traditional empirical kinetic model
169 approach (EKMA) (Dodge et al., 1977), the OH reactivity due to VOCs (termed as
170 VOCs reactivity) rather than VOCs mixing ratio was used in the calculation of ozone
171 production rate (Geddes et al., 2009; LaFranchi et al., 2011; Sinha et al, 2012; Zhang
172 et al., 2014). Due to the limitation of current measurement techniques, some VOCs
173 species which could not be quantified so far, and therefore cannot be integrated into
174 current chemical mechanisms of model run, could laid a great uncertainty in ozone
175 production prediction. By directly measuring the total OH reactivity, VOCs reactivity
176 can be obtained by deducting the inorganic reactivity from the total OH reactivity,
177 which provides a constrain for evaluating the roles of reactive VOCs in air chemistry
178 (Sadanaga et al, 2005; Sinha et al, 2012; Yang et al., 2016).

179 This paper presents field data in China from two intensive observation conducted
180 in August 2013 in Beijing, and October to November 2014 in Heshan, Guangdong,
181 focusing on OH reactivity and related species. The variations of total OH reactivity at
182 both sites were compared with similar observations in urban and suburban areas
183 worldwide. Thereafter, a zero dimensional box model based on Regional Atmospheric
184 Chemical Mechanism 2 (RACM2) was employed for OH reactivity simulations. The
185 possible missing reactivity and its importance for the ozone production calculation are
186 discussed.

187

188 **2. Methods**

189 **2.1 Total OH reactivity measurements**

190 **2.1.1 Measurement principles**

191 Total OH reactivity was measured by the comparative reactivity method (CRM)
192 first developed at Max Planck Institute for Chemistry (Sinha et al., 2008). The CRM
193 system was built accordingly in Peking University, which consisted of 3 major
194 components: inlet and calibration system, reactor, and measuring system as shown in

195 Fig 1. Ambient air was sampled after a teflon filter and then pumped through a 14.9m
196 Teflon 3/8 inch (outer diameter) inlet at about $7 \text{ L} \cdot \text{min}^{-1}$ rate, with a 5 - 6 s residence
197 time.

198 In this method, pyrrole ($\text{C}_4\text{H}_5\text{N}$) was used as the reference substance and was
199 quantified by a quadrupole PTR-MS (Ionicon Analytic, Austria). There are 4 working
200 modes for measuring procedure: In the C0 mode, pyrrole (Air Liquid Ltd, U.S.) is
201 introduced into the reactor with dry synthetic air (99.99%, Chengweixin Gas Ltd,
202 China). A mercury lamp (185nm, used for OH radicals generation) is turned off and
203 high-pure dry nitrogen (99.99%, Chengweixin Gas Ltd, China), is mixed into the
204 reactor through a second arm. In this mode, the highest signals of m/z 68 (protonated
205 mass of pyrrole) c_0 are obtained. Then in the C1 mode, the nitrogen and synthetic air
206 is still dry but the mercury lamp is turned on. The mixing ratio of pyrrole decreased to
207 c_1 . The difference between c_0 and c_1 is mainly due to the photolysis of pyrrole (Sinha
208 et al., 2008). C2 mode is the “zero air” mode in which synthetic air and nitrogen are
209 humidified before being introduced into the reactor. The photolysis of water vapor
210 generates OH radicals which react with pyrrole in the reactor to c_2 level. Then C3
211 mode is the measuring mode in which the automatic valve switches from synthetic air
212 to ambient air. The ambient air is pumped into the reactor to react with OH radicals,
213 competing with pyrrole molecules. The mixing ratio of pyrrole is detected as c_3 . Total
214 OH reactivity is calculated as below, based on equations from Sinha et al. (2008):

$$k_{OH} = c_1 \times k_{Pyr+OH} \times \frac{c_3 - c_2}{c_1 - c_3} \quad (2-1)$$

216 Ambient air or synthetic air was introduced at $160 - 170 \text{ ml min}^{-1}$ with the total
217 flow $320 - 350 \text{ ml min}^{-1}$ (The typical dilution factor was about 2-2.15 depending on
218 the situation). The residence time of air inside the reactor was less than 30 s before
219 they were pumped by the Teflon pump. The typical c_1 mixing ratio for pyrrole in
220 Beijing and Heshan measurements were about 60 ppbV and 55 ppbV, while the
221 mixing ratios of OH radicals generated by mercury lamp were about 35 ppbV and 28
222 ppbV. The mixing ratios were quite consistent for either of the campaigns,
223 respectively. Corrections about pseudo-first order kinetics were conducted for both

224 measurements, based on the methods in Sinha et al (2008). The typical correction
225 factors could be presented as

226 $R_{\text{true}} = 0.0008 * (R_{\text{mea}})^2 + 0.78 * R_{\text{mea}} - 0.042$ (2-2)

227 $R_{\text{true}} = -0.0004 * (R_{\text{mea}})^2 + 0.81 * R_{\text{mea}} - 0.017$ (2-3)

228 **2.1.2 Calibrations and tests**

229 We performed two calibrations for the measurements. First, PTR-MS was
230 calibrated by diluted dry pyrrole standard gas ranging from less than 10 ppbV to over
231 160 ppbV (presented in Fig S1). Additionally, we conducted an inter-comparison with
232 humidified pyrrole dilution gas. The sensitivity was about 3% to 5% higher than dry
233 calibration, which was considered for later calculation (Sinha et al., 2009). The tests
234 of the CRM system were done by using both the single standard gas, such as CO,
235 propane, propene (Huayuan Gas Ltd, China) and a standard of the mixture of 56
236 non-methane hydrocarbons (NMHCs) (SpecialGas Ltd, U.S.). The results of the
237 calibrations and tests were presented in Fig 2. Measured and calculated OH reactivity
238 agreed well within the uncertainty for all calibrations.

239 A key factor influencing the measurement results is the stability of OH radical
240 generator. One major interference could be the difference in relative humidity
241 between C2 mode and C3 mode. During the experiment, we used one single needle
242 valve to control the flow rate of synthetic air going through the bubbler, so that the
243 relative humidity during C2 mode could be adjusted to match humidity during
244 ambient sampling (C3 mode). Meanwhile, the remaining minor difference could be
245 corrected by factors derived from the OH reactivity-humidity correction experiment.
246 The details of the OH-correction experiment and the data were presented in the
247 supporting information (Fig. S1 and S2).

248 The other interference might be caused by ambient NO, which produces
249 additional OH radicals via recycling of HO₂ radicals (Sinha et al., 2008; Dolgorouky
250 et al., 2012; Michoud et al., 2015). The amount of OH radical through this pathway is
251 hard to be quantified. In the morning rush hours or on polluted cloudy days, NO
252 levels could rise to over 30 ppbV in both Beijing and Heshan, which could then
253 potentially introduce high uncertainties for measurements. The NO-correction

254 experiments were conducted by introducing given amounts of VOCs standard gases
255 into the reactor. When the stable concentrations for c2 were reached, different levels
256 of NO were injected into the reactor and the “measured” reactivity decreased as the
257 NO mixing ratio increased. Then a correction curve was fitted between the differences
258 in reactivity and NO mixing ratios. Several standard gases and different levels of base
259 reactivity (from less than 30s^{-1} to over 180s^{-1}) have been tried and the curve was quite
260 consistent for all tested gases, as shown in Fig 3. The correction derived from the
261 curve was used later to correct ambient measurements according to simultaneous
262 detected NO levels. The correction was necessary when NO mixing ratio was larger
263 than 5 ppbV, which was quite often observed in the morning time as well as cloudy
264 days in Beijing and Heshan. The relative change for reactivity results could be over
265 100s^{-1} when NO mixing ratio was about 30 ppbV.

266 A further potential interference comes from nitrous acid (HONO). The photolysis
267 of HONO in the reactor could generate the same amount of OH radicals and NO
268 molecules, as shown in R1. The additional OH radicals and NO molecules can be both
269 interferences with the reactivity measurements. Similar correction experiments were
270 conducted as the NO correction experiment. HONO were added stepwise in several
271 mixing ratios (1-10 ppbV), generated by a HONO generator (Liu et al., 2016) and
272 thus introduced into the reactor. A curve was fitted between the differences in
273 reactivity and HONO mixing ratios, as presented in Fig 4. The correction associated
274 with this curve was also applied later in the ambient measurements.



276 To make sure the production of OH radicals was stable during the experiments,
277 C1 mode was measured for 1-2 hour every other day and C2 mode was measured for
278 20-30 minutes every two hours. With above calibrations and tests into consideration,
279 the detection limits of CRM methods in two campaigns was around 5s^{-1} (2σ). The
280 total uncertainty of the method was about 20% (1σ), due to rate coefficient of pyrrole
281 reactions (15%), flow fluctuation (3%), instrument precision (6% when measured
282 reactivity $> 15\text{s}^{-1}$), standard gases (5%) and corrections for relative humidity (5%).

283

284 **2.2 Field measurements**

285 **2.2.1 Measuring sites and periods**

286 The urban measurements started from August 10th to August 27th, 2013 at Peking
287 University (PKU) Site (116.18°E, 39.99°N), which was set on the roof of a 6-floor
288 building. The site is about 300 m from the 6-lanes road to the east and 500 m to the 8
289 -lanes road to the south. This site is an urban site used for intensive field
290 measurements of air quality in Beijing for long. Detailed information about this site
291 can be found elsewhere (Yuan et al., 2012).

292 Suburban measurements were conducted from October 20th to November 22nd
293 2014 at Heshan (HS) site, Guangdong (112.93°E, 22.73°N). The site is located on top
294 of a small hill (60 m above ground) in Jiangmen, which is 50km from a medium size
295 city Foshan (with a population of about 7 million) and 80 km from a megacity
296 Guangzhou. This is the super-site for measurements of air quality trends by
297 Guangdong provincial government, detailed information about which can also be
298 found in Fang et al (2016).

299 **2.2.2 Simultaneous measurements**

300 During both intensive campaigns, fundamental meteorological parameters and
301 trace gases were measured simultaneously. Meteorological parameters, such as
302 temperature, relative humidity, pressure, wind speed, wind direction were measured.
303 NO and NO_x mixing ratios were measured by chemi-luminescence (model 42i,
304 Thermo Fischer Inc, U.S.), and O₃ was measured by UV absorption (model 49i,
305 Thermo Fischer Inc, U.S.). CO was measured by Gas Filter Correlation (model 48i,
306 Thermo Fischer Inc, U.S.), and SO₂ was measured by pulsed fluorescence (model 43C,
307 Thermo Fischer Inc, U.S.). The photolysis frequencies were measured by a spectral
308 radiometer (SR) including 8 photolysis parameters. These parameters were all
309 averaged into 1-minute resolution. The performances of these instruments were
310 presented in Table S1 and Table S2.

311 VOCs were measured by a cryogen-free online GC-MSD/FID system, developed
312 by Peking University (Yuan et al., 2012; Wang et al., 2014a). The time resolution is 1

313 hour but the sampling time starts from the 5th minute to 10th minute every hour. The
314 system was calibrated by two sets of standard gases: 56 NMHCs including 28 alkanes,
315 13 alkenes and alkynes, 15 aromatics; EPA TO-15 standards
316 (<http://www.epa.gov/ttnamti1/les/ambient/airtox/to-15r.pdf>), including additional
317 OVOCs and halocarbons. The detection limits ranged from 10ppt-50ppt, depending
318 on the species. Formaldehyde was measured by the Hantzsch method with time
319 resolution of 1 minute. Detailed information about this instrument is described in one
320 previous paper (Li et al., 2014).

321 **2.3 Model description**

322 **2.3.1 Box model**

323 A zero-dimensional box model was applied to produce the unmeasured secondary
324 products and OH reactivity for both field observations. The chemical mechanism
325 employed in the model was RACM2 (Stockwell et al., 1997, Goliff et al., 2013), with
326 implementation of Mainz Isoprene Mechanism (MIM, Pöschl et al., 2000) and update
327 versions by Geiger et al. (2003) and Karl et al. (2006) for isoprene reactions. The
328 model was constrained by measured photolysis frequencies, ancillary meteorology
329 and inorganic gases measurements, as well as VOCs data. Mixing ratios of methane
330 and H₂ were set to be 1.8 ppmV and 550 ppbV. The model was calculated in a
331 time-dependent mode with 5-min time resolution. Each model run started with 3 days
332 spin-up time to reach steady-state conditions for long-lived species. Different
333 scenarios with 1 day, 2 days and 3 days spin-up time have been tried while the
334 differences were within 10%. Additional loss by dry deposition was assumed to have
335 a corresponding lifetime of 24 hours to avoid the accumulation of secondary
336 productions. The boundary layer height was set as constant as 1000 m in the model
337 due to the lack in measurements. This was similar to model setups in Lu et al (2013)
338 and field measurement results in Guo et al (2016).

339 **2.3.2 Ozone production efficiency**

340 Ozone production efficiency (OPE) is defined as the number of molecules of
341 total oxidants produced photochemically when a molecule of NO_x was oxidized
342 (Kleinman, 2002, Chou et al., 2011). It helps to evaluate the impacts of VOCs

343 reactivity on ozone production in various NO_x regimes. In this work, the OPE was
344 expressed as the ratio of ozone production rate (i.e. P(O₃)) to NO_x consumption rate
345 (i.e. D(NO_x)). NO_z, calculated as the difference between NO_y (sum of all odd-nitrogen
346 compounds) and NO_x, was assumed to be the oxidation products of NOx. Thus the
347 OPE could be also calculated as P(O₃)/P(NO_z). The ozone production rate is obtained
348 as 2-2, and the P(NO_z) is approximately as production rate of HNO₃ as well as the
349 production rate of organic nitrate, which is given as 2-3.

$$350 \quad P(O_3) = k_{HO_2+NO} [HO_2][NO] + \sum_i k_{RO_{2i}+NO} [RO_{2i}][NO] \quad (2-2)$$

$$351 \quad P(NO_z) = k_{NO_2+OH} [NO_2][OH] + \sum_i k_{RO_i+NO_2} [RO_i][NO_2] \quad (2-3)$$

352 **3. Results**

353 **3.1 Time series of meteorology and trace gases**

354 The time series of selected meteorological parameters and inorganic trace gases
355 were presented in 5 minute averages (Fig 5). The median values of the inorganic trace
356 gases were 0.715 ± 0.335 ppmV for CO, 6.3 ± 5.75 ppbV for NO and 36.5 ± 21.3
357 ppbV for NO₂, 57 ± 44 ppbV for O₃ in Beijing. In Heshan, the median results were
358 0.635 ± 0.355 ppmV for CO, 9.7 ± 6.95 ppbV for NO, 29.6 ± 12.6 ppbV for NO₂, and
359 55.7 ± 34.9 ppbV for O₃. Both results were within the range of data from literatures
360 (Zhang et al., 2008; Zheng et al., 2010; Zhang et al., 2014). However, daytime
361 averaged O₃ mixing ratio in Beijing 2013 was a little lower than the medium results
362 (about 60 ppbV) in normal years (Zhang et al., 2014). This could be due to higher
363 frequencies of cloudy and rainy days, which accounted for about 1/3 of our
364 measurement duration. The measured maximum photolysis rates in cloudy/rainy days
365 were about half of peak values of J(O¹D) on sunny days. Even under this
366 circumstances, ozone levels from the campaign remained high, the pollution episodes
367 with ozone exceeding Grade II of China National Ambient Air Quality Standards (93
368 ppbV) occurred quite often, and the percentage of exceedance were 40% in Beijing
369 and 20% in Heshan.

370 The mixing ratios of VOCs in both campaigns were presented in Table S3 and
371 Table S4. In summer Beijing, alkanes accounted for over 60% of the summed VOCs

mixing ratios during most of the time, while in Heshan the contribution from aromatics was 6% higher than that in Beijing. This could be explained by stronger emissions from solvent use and paint industry in the PRD region (Zheng et al., 2009). The ratio of toluene to benzene, which is typically used qualitatively as an indicator for aromatics emission sources also supported this assumption. While this ratio in Beijing was close to 2, similar to vehicle emissions (Barletta et al., 2005), the ratio in Heshan was higher than 3 due to strict control of benzene in solvent usage these days (Barletta et al., 2005; Liu et al., 2008). In the ozone polluted episode in Fig 5, the mixing ratios of most species were about twice to three times higher than the daily average results.

The diurnal variations of NO_x, O₃ and photochemical age from Beijing and Heshan site were compared in Fig 6 and Fig 7. Both sites presented similar diurnal patterns for O₃ and NO. However, the highest 1-hour average O₃ value at PKU site came in the afternoon and stayed at high level till the dawn. While O₃ pattern at Heshan site did not stay high in the afternoon. An additional similarity was that the NO peaks occurred at similar times for both sites. But NO decreased at a slower rate in Heshan till even 12:00 p.m. This was likely explained by the facts that the NO observed at PKU site was mainly from local vehicle emissions while NO_x at Heshan site was significantly influenced by long-range transported of air masses.

VOCs measurements provided us chance to evaluate the oxidation state at two sites. Based on the OH exposure calculation methods (de Gouw et al., 2005), we chose a pair of VOCs species: m,p-xylene and ethylbenzene to calculate the photochemical age:

$$[\text{OH}]\Delta t = [\ln(\frac{[E]}{[X]})_t - \ln(\frac{[E]}{[X]})_0]/(k_E - k_x) \quad (3-1)$$

Here, [E] and [X] represents the mixing ratios of ethylbenzene and m,p-xylene, k_E and k_x means the OH reaction rate coefficient of ethylbenzene and m,p-xylene. As presented in Fig 7, we chose 1.15 ppbV ppbV⁻¹ and 2.3 ppbV ppbV⁻¹ as emission ratios of ethylbenzene to m,p-xylene in Beijing and Heshan, as they were the largest ratios in diurnal variations for the campaign. The largest OH exposure in Beijing 2013

401 was calculated as 0.71×10^{11} molecule s cm⁻³ in 13:00 LTC, while the largest OH
402 exposure in Heshan 2014 was calculated to be 1.69×10^{11} molecule s cm⁻³ in 14:00
403 LTC. The results in Beijing were comparable to previous reports (Yuan et al., 2012).
404 Assuming the daytime average ambient OH concentration was 5.2×10^6 molecule
405 cm⁻³ (Lu et al., 2013), the photochemical age in Beijing was estimated to be not more
406 than 3.5 h. With measured daytime average OH concentration as 7.5×10^6 molecule
407 cm⁻³ in Heshan (Tan et al., in preparation), the photochemical age in Heshan was
408 about 6 h to 7 h, which was about twice the photochemical age of the Beijing
409 observations, indicating a more aged atmospheric environment in Heshan. However,
410 the assumed OH radical concentrations' influence on the photochemical age results
411 should not be neglected.

412 **3.2 Measured reactivity**

413 Total OH reactivity ranged from less than 10 s⁻¹ to over 100 s⁻¹ in Beijing (Fig
414 5a). The daily median value was 20 ± 11 s⁻¹. The diurnal patterns changed
415 significantly from day to day (Fig 8). The averaged diurnal pattern showed that the
416 total OH reactivity was higher from dawn to morning rush hours with a peak hourly
417 mean of 27 s⁻¹, and decreased to a lower value, median value of 17 s⁻¹ in the afternoon.
418 This diurnal pattern was similar to the variations of NO_x mixing ratios (Williams et al.,
419 2016).

420 Meanwhile, measured total OH reactivity in Heshan was higher in median but
421 the diel variation was less evident. The daily median value was 31 ± 20 s⁻¹. The OH
422 reactivity was much less variable in the daily variation. This could possibly due to the
423 more aged air masses in Heshan, as presented in 3.1. The other probable explanation
424 could be the two periods of clean air we encountered, during which ground-level
425 ozone and PM_{2.5} concentrations were rather low, each of the cases lasted for about 5
426 days during our measurements. And 2 pollution episodes were identified between
427 October 24th to 27th and November 14th to 17th, 2014. Both episodes showed
428 accumulation of ozone and PM_{2.5}. The total OH reactivity level also built up
429 significantly (Fig 5b).

430 **3.3 Variations in missing reactivity**

431 Significant differences were found between the measured reactivity and
432 calculated reactivity which derived from mixing ratios of different species multiplied
433 by their rate coefficients with OH radicals, as presented in Fig 5a for Beijing and Fig
434 5b for Heshan. Taking all measured species into consideration, NO_x and NMHCs
435 showed the largest contribution, 45%-55% of total OH reactivity (Fig 9). The OVOCs
436 had also significant contribution, and measured OVOCs had a sharing of 10% in total
437 reactivity in Beijing while 7% in Heshan.

438 The Missing reactivity was on average over 4 s⁻¹, 21 ± 17 % of the total OH
439 reactivity in Beijing and 10 s⁻¹, 32 ± 21% in Heshan. The missing reactivity presented
440 different temporal patterns. In Beijing, the missing reactivities were high during
441 pollution episodes, especially in the morning rush hours. The percentage of missing
442 reactivity could reach over 50%. For the Heshan site, the missing reactivity was more
443 or less stable during the entire campaign. Even in clean days with reactivity levels
444 lower than 20 s⁻¹, 20%-30% of missing reactivity still existed.

445 **4. Discussion**

446 **4.1 Reactivity levels in Beijing and Heshan**

447 The measured VOCs reactivity (obtained by subtracting inorganic reactivity from
448 total OH reactivity), 11.2 s⁻¹ in Beijing and 18.3 s⁻¹ in Heshan (Fig 10), was actually
449 not at high end comparing with the levels from literatures. Tokyo presented a similar
450 level of VOCs reactivity (Yoshino et al., 2006). The measured NMHCs levels
451 (obtained by adding all hydrocarbon mixing ratios together) were also not very high,
452 with Beijing 2013 being around 20 ppbV and Heshan 2014 higher than 35 ppbV. The
453 relative VOCs reactivity, defined by the ratio of the VOCs reactivity to the measured
454 NMHCs levels, the values for both Beijing and Heshan were very high.

455 One possible explanation is the higher content of reactive hydrocarbons in China.
456 Compared to other campaigns, both sites had higher loading of alkenes and aromatics
457 (Yuan et al., 2012; Wang et al., 2014b). The other probable reason is the contribution
458 from OVOCs. In Beijing and Heshan, ambient formaldehyde could accumulate to
459 over 10 ppbV, which was significantly higher than levels found in other observations

460 (Li et al., 2013; Chen et al., 2014). Another possible explanation is unmeasured
461 species, either primary hydrocarbons or secondary products, which will be discussed
462 in later sessions.

463 **4.2 Contributions to the missing reactivity: primary VOCs**

464 As missing reactivity was observed at Beijing and Heshan site, the species
465 possibly causing these missing were examined. Throughout the whole campaign at the
466 PKU site, missing reactivity was normally found in the morning, as for an example in
467 August 16th and 17th 2013 in (Fig 11). Between 5 a.m. to 10 a.m., local vehicle-related
468 sources were strong, and the chemical reactions were not active yet, and the oxidants
469 levels thus the secondary VOC species remained low. We assumed that the
470 unmeasured primary VOCs species could most likely be the major contributors to
471 missing reactivity. Special attention was paid to the unmeasured branched-alkenes for
472 their high reactivity and was previously observed from vehicle exhaust (Nakashima et
473 al., 2010) and gasoline evaporation emissions (Wu et al., 2015). We found only one
474 dataset of branched alkenes measurements in Beijing, 2005 measured by NOAA (Liu
475 et al., 2009). We chose the diurnal patterns of missing reactivity in Beijing in 2013
476 and compared to the diel cycles of four measured branched-alkenes in 2005. The
477 correlations were found as presented in Fig 11. Considering the contribution of the 4
478 branched alkenes, the VOCs reactivity could be enhanced by 2.3 s⁻¹. This could only
479 partially explain the missing VOCs reactivity which was around 10 s⁻¹. With observed
480 decreasing trends in mixing ratios of most NMHCs species in Beijing (Zhang et al.,
481 2014; Wang et al., 2015), the branched-alkenes were insufficient to tell the full story
482 of the missing reactivity. Unmeasured semi-volatile organic compounds (SVOCs) and
483 intermediate volatile organic compounds (IVOCs), such as alkanes between C12 to
484 C30, and polycyclic aromatic hydrocarbons (PAHs) could be also important. Sheehy
485 (2010) found SVOCs and IVOCs contributed to about 10% in morning time in
486 Mexico City. Future studies with a wider range of reactive VOCs measurement for
487 total OH reactivity closure is needed.

488 **4.3 Contributions to the missing reactivity: secondary VOCs**

489 Due to limitations in chemistry mechanisms as well as measuring techniques,

secondary products are not fully quantified in ambient air and could probably contribute significantly to the observed missing reactivity, especially in the urban or suburban sites receiving chemically complex aged air masses.

Besides the large missing reactivity during the morning rush hour, there was about 25% difference between measured and calculated reactivity from August 16th to 18th, 2013 at PKU site. Considering high levels of oxidants in daytime, the mixing ratios of branched-alkenes could be lower than 0.1 ppbV, which could not explain the observed missing reactivity. A box model was deployed to investigate the role of secondary species in variation of VOCs reactivity. The model, constrained by measured parameters (meteorology, inorganic gases, VOCs including measured carbonyls), gave the results of VOCs reactivity which agreed well with the measured reactivity in most of the daytime (Fig 11). Major contributors from modeled species were unmeasured aldehydes, glyoxal and methyl glyoxal. Average values of major secondary contributors to modelled reactivity were provided in Table S5. However, the missing in morning hours remain unsolved: In the model run, the higher secondary contribution on August 17th 2013 morning was owing to isoprene oxidation products, by using 1.5 ppbv of isoprene levels as model input, the missing reactivity kept over 40% around 7:00 and 8:00 a. m.

The similar model was applied for the Heshan observation (Fig 12). During the polluted episode between October 24th and 27th 2014, a 30% missing reactivity existed for most time. Unfortunately, the modeled reactivity was only 10-20% higher than calculated reactivity, and not enough to explain the measured reactivity. The major contributors among modeled species were also unmeasured aldehydes, glyoxal, methyl glyoxal and other secondary products, as shown in Table S6. Due to strong emissions of aromatics from solvent use and petroleum industry in PRD region (Zheng et al., 2009), high levels of glyoxal and methyl glyoxal in this region were observed from satellite measurement (Liu et al., 2012) and ground measurements (Li et al., 2013). Compared to the 2006 measurements in Back garden, a semi-rural site in PRD region, the modeled glyoxal was twice as high as around 0.8 ppbV (Li et al., 2013). This difference possibly resulted from higher levels of precursors in 2014

520 measurements, where the measured reactivity was about 50% higher than the results
521 in Backgarden 2006 (Lou et al., 2010).

522 **4.4 Implications for ozone production efficiency**

523 The investigating of missing in VOCs reactivity is expected to better understand
524 the ozone formation processes. To evaluate this contribution, we employed the box
525 model to calculate the influence of VOCs reactivity on OPE. We set two scenarios for
526 the model run: 1) The base run was constrained with measured species, including all
527 inorganic compounds, PAMS 56 hydrocarbons, TO-15 OVOCs and formaldehyde.
528 This is how we obtained the modelled reactivity as presented above, and the
529 intermediates and oxidation products were reproduced as well. 2) The other scenario
530 used measured reactivity as a constraint. Due to the difference between measured and
531 modeled reactivity, we allocated the missing reactivity into several groups. For the
532 primary species, we assumed the ratio between total chain-alkenes and
533 branched-alkenes were the same in Beijing 2013 and in Heshan 2014 as the ratio in
534 Beijing 2005, so we got the assumed mixing ratios of branched-alkenes at both sites.
535 For secondary species, we allocated the remaining missing reactivity into different
536 intermediates or products based on weights obtained in the model base run. Under
537 both assumptions, we ran the OBM and calculated the OPE, as presented in Fig 13.

538 For both sites, the OPE constrained by measured reactivity were significantly
539 higher than the OPE we calculated from modeled reactivity. In Beijing, the OPE from
540 measured reactivity was about 21% higher on average. The value was 30% higher at
541 Heshan site under similar assumptions. This percentage was close to the percentage of
542 missing reactivity, indicating the ignorance of unmeasured or unknown organic
543 species can cause significant underestimation in ozone production calculation. When
544 the four branched-alkenes were included in the OPE calculation, the OPE results
545 would be 4% higher than the OPE constrained by calculated reactivity, but still far
546 from the OPE constrained by measured reactivity.

547 Compared to other similar calculations worldwide, the OPE results for Beijing
548 and Heshan were significantly higher (Fig 14). The comparison was made for NO_x =
549 20 ppbV which was in the range of most observation results. For urban measurements,

550 only the results from Mexico City in MCMA-03 were close to the Beijing results in
551 basic model run (Lei et al., 2008). For suburban measurements, the OPE in Heshan
552 2014 was higher than all other three campaigns, even including the results from
553 Shangdianzi station in CAREBEIJING-2008 campaigns (Ge et al., 2012). While
554 taking missing reactivity into consideration, the OPE results were even higher,
555 indicating more ozone was produced by the reactions of the same quantity of NO_x
556 molecules.

557 **5. Conclusions**

558 In this study, total OH reactivity measurements employing CRM system were
559 conducted at PKU site in Beijing 2013, and Heshan site 2014 in PRD region.
560 Comparisons between measured and calculated, as well as modelled reactivity were
561 made and possible reasons for the missing reactivity have been investigated. The
562 contribution of missing reactivity to ozone production efficiency was evaluated.

563 In Beijing 2013, daily median result for measured total OH reactivity was $20 \pm$
564 11 s^{-1} . Similar diurnal variation with other urban measurements was found with peaks
565 over 25 s^{-1} during the morning rush hour and lower reactivity than 16 s^{-1} in the
566 afternoon. In Heshan 2014, total OH reactivity was $31 \pm 20 \text{ s}^{-1}$ on daily median result.
567 The diurnal variation was not significant. Both sites have experienced OH reactivity
568 over 80 s^{-1} during polluted episodes.

569 Missing reactivity was found at both sites. While in Beijing the missing
570 reactivity made up 21% of measured reactivity, some periods even reached a higher
571 missing percentage as 40%-50%. In Heshan, missing reactivity's contribution to total
572 OH reactivity was 32% on average and quite stable for the whole day. Unmeasured
573 primary species, such as branched-alkenes could be important contributor to the
574 missing reactivity in Beijing, especially in morning rush hour, but they were not
575 enough to explain Aug 17th morning's event. With the help of RACM2, unmeasured
576 secondary products were calculated and thus the modelled reactivity could agree with
577 measured reactivity in Beijing in the noontime. However, they were still not enough
578 to explain the missing reactivity in Heshan, even in daytime. This was probably

579 because of the relatively higher oxidation stage in Heshan than in Beijing.

580 Missing reactivity could impact the estimation of atmospheric ozone production
581 efficiency. Compared to modeled reactivity from base run, ozone production
582 efficiency would rise 21% and 30% in Beijing and Heshan with measured reactivity
583 applied. Both results were significantly higher than similar observations worldwide,
584 indicating the relatively faster ozone production at both sites.

585 However, in order to further explore the OH reactivity in both regions, more
586 efforts should be paid in both OH reactivity measurements and speciated
587 measurements, as well as modeling to close the total OH reactivity budget. Moreover,
588 a thorough way with more detailed mechanisms should be established to connect the
589 missing reactivity to the evaluation of ozone production.

590

591 **Acknowledgement**

592 This study was funded by the National Key Research and Development Plan (grant no.
593 2016YFC020200), Natural Science Foundation for Outstanding Young Scholars
594 (grant no. 41125018) and a Natural Science Foundation key project (grant
595 no.411330635). The research was also supported by the European Commission
596 Partnership with China on Space Data (PANDA project). Special thanks to Jing Zheng,
597 Mei Li, Yuhua Liu from Peking University and Tao Zhang from Guangdong
598 Environmental Monitoring Center for the help, thanks for William. C. Kuster from
599 NOAA . Earth System Research Laboratory for the branched-alkenes data in 2005.

600

601

602

603

604

605

606

607

608

609 **Reference**

- 610 Barletta, B., Meinardi, S., Sherwood Rowland, F., Chan, C.-Y., Wang, X., Zou, S., Yin
611 Chan, L., and Blake, D. R.: Volatile organic compounds in 43 Chinese cities, *Atmos.*
612 *Environ.*, 39, 5979-5990, doi: 10.1016/j.atmosenv.2005.06.029, 2005.
- 613 Calpini, B., Jeanneret, F., Bourqui, M., Clappier, A., Vajtai, R., and van den Bergh, H.:
614 Direct measurement of the total reaction rate of OH in the atmosphere, *Analusis*, 27,
615 328-336, doi: 10.1051/analusis:1999270328, 1999.
- 616 Chatani, S., Shimo, N., Matsunaga, S., Kajii, Y., Kato, S., Nakashima, Y., Miyazaki,
617 K., Ishii, K., and H., U.: Sensitivity analyses of OH missing sinks over Tokyo
618 metropolitan area in the summer of 2007, *Atmos. Chem. Phys.*, 9, 8975-8986, doi:
619 10.5194/acp-9-8975-2009, 2009.
- 620 Chen, W. T., Shao, M., Lu, S. H., Wang, M., Zeng, L. M., Yuan, B., Liu, Y.:
621 Understanding primary and secondary sources of ambient carbonyl compounds in
622 Beijing using the PMF model. *Atmos. Chem. Phys.*, 14, 3047-3062, doi:
623 10.5194/acp-14-3047-2014, 2014.
- 624 Chou, C. C. K., Tsai, C. Y., Chang, C. C., Lin, P. H., Liu, S. C., and Zhu, T.:
625 Photochemical production of ozone in Beijing during the 2008 Olympic Games,
626 *Atmos. Chem. Phys.*, 11, 9825-9837, doi: 10.5194/acp-11-9825-2011, 2011.
- 627 Dodge, M. C.: Proceedings of the international conference on photochemical oxidant
628 pollution and its control. Combined use of modeling techniques and smog chamber
629 data to derive ozone-precursor relationships, U.S. Environmental Protection Agency,
630 Research Triangle Park, NC, 881-889 pp., 1977.
- 631 de Gouw, J. A., Middlebrook, A. M., Warneke, C., Goldan, P. D., Kuster, W. C.,
632 Roberts, J. M., Fehsenfeld, F. C., Worsnop, D. R., Canagaratna, M. R., Pszenny, A. A.
633 P., Keene, W. C., Marchewka, M., Bertman, S. B., Bates, T. S.: Budget of organic
634 carbon in a polluted atmosphere: Results from the New England Air Quality Study in
635 2002, *J. Geophy. Res.-Atmos.*, 110, D16305, doi: 10.1029/2004jd005623, 2005.
- 636 Dolgorouky, C., Gros, V., Sarda-Esteve, R., Sinha, V., Williams, J., Marchand, N.,
637 Sauvage, S., Poulain, L., Sciare, J., and Bonsang, B.: Total OH reactivity
638 measurements in Paris during the 2010 MEGAPOLI winter campaign, *Atmos. Chem.*
639 *Phys.*, 12, 9593-9612, doi: 10.5194/acp-12-9593-2012, 2012.
- 640 Edwards, P. M., Evans, M. J., Furneaux, K. L., Hopkins, J., Ingham, T., Jones, C., Lee,
641 J. D., Lewis, A. C., Moller, S. J., Stone, D., Whalley, L. K., and Heard, D. E.: OH

reactivity in a South East Asian tropical rainforest during the Oxidant and Particle Photochemical Processes (OP3) project, *Atmos. Chem. Phys.*, 13, 9497-9514, doi: 10.5194/acp-13-9497-2013, 2013.

Fang, X., Shao, M., Stohl, A., Zhang, Q., Zheng, J., Guo, H., Wang, C., Wang, M., Ou, J., Thompson, R. L., and Prinn, R. G.: Top-down estimates of benzene and toluene emissions in the Pearl River Delta and Hong Kong, China, *Atmos. Chem. Phys.*, 16, 3369-3382, doi: 10.5194/acp-16-3369-2016, 2016.

Fuchs, H., Hofzumahaus, A., Rohrer, F., Bohn, B., Brauers, T., Dorn, H. P., Häseler, R., Holland, F., Kaminski, M., Li, X., Lu, K., Nehr, S., Tillmann, R., Wegener, R., and Wahner, A.: Experimental evidence for efficient hydroxyl radical regeneration in isoprene oxidation, *Nature Geoscience*, 6, 1023-1026, doi: 10.1038/ngeo1964, 2013.

Fuchs, H., Tan, Z. F., Lu, K. D., Bohn, B., Broch, B., Brown, S. S., Dong, H. B., Gomm, S., Haseler, H. L. Y., Hofzumahaus, A., Holland, F., Li, X., Liu, Y., Lu, S. H., Min, K.-E., Rohrer, F., Shao, M., Wang, B. L., Wang, M., Wu, Y. S., Zeng, L. M., Zhang, Y. S., Wahner, A., Zhang, Y. H.: OH reactivity at a rural site (Wangdu) in the North China Plain: Contributions from OH reactants and experimental OH budget, *Atmos. Chem. Phys. Dis.*, 716-745, doi: 10.5194/acp-2016-716, 2016.

Ge, B. Z., Sun, Y. L., Liu, Y., Dong, H. B., Ji, D. S., Jiang, Q., Li, J., Wang, Z. F.: Nitrogen dioxide measurement by cavity attenuated phase shift spectroscopy (CAPS) and implications in ozone production efficiency and nitrate formation in Beijing, China. *J. Geophys. Res.-Atmos.*, 118, 9499-9509, doi: 10.1002/jgrd.50757, 2013.

Geddes, J. A., Murphy, J. G., and K., W. D.: Long term changes in nitrogen oxides and volatile organic compounds in Toronto and the challenges facing local ozone control, *Atmos. Environ.*, 43, 3407-3415, doi: 10.1016/j.atmosenv.2009.03.053, 2009.

Geiger, H., Barnes, I., Bejan, I., Benter, T., and Spittler, M.: The tropospheric degradation of isoprene: an updated module for the regional atmospheric chemistry mechanism, *Atmos. Environ.*, 37, 1503–1519, doi: 10.1016/S1352-2310(02)01047-6, 2003.

Goliff, W. S., Stockwell, W. R., Lawson, C. V.: The regional atmospheric chemistry mechanism, version 2. *Atmos. Environ.*, 68, 174-185, doi: 10.1016/j.atmosenv.2012.11.038, 2013

Guo, J. P., Miao, Y. C., Zhang, Y., Liu, H., Li, Z. Q., Zhang, W. C. He, J., Lou, M. Y., Yan, Y., Bian, L. G., Zhai, P. M.: The climatology of planetary boundary layer height in China derived from radiosonde and reanalysis data., *Atmos. Chem. Phys.*, 16,

- 676 13309-13319, doi: 10.5194/acp-16-13309-2016, 2016
- 677 Hansen, R. F., Blocquet, M., Schoemaecker, C., Léonardis, T., Locoge, N., Fittschen,
678 C., Hanoune, B., Stevens, P. S., Sinha, V., and Dusanter, S.: Intercomparison of the
679 comparative reactivity method (CRM) and pump–probe technique for measuring total
680 OH reactivity in an urban environment, *Atmos. Meas. Tech.*, 8, 4243-4264, doi:
681 10.5194/amt-8-4243-2015, 2015.
- 682 Ingham, T., Goddard, A., Whalley, L. K., Furneaux, K. L., Edwards, P. M., Seals, C. P.,
683 Self, D. E., Johnson, G. P., Read, K. A., Lee, J. D., and E., H. D.: a flow tube based
684 LIF instrument to measure OH reactivity in the troposphere, *Atmos. Meas. Tech.*, 2,
685 465-477, doi: 10.5194/amt-2-465-2009, 2009.
- 686 Karl, M., Dorn, H.-P., Holland, F., Koppmann, R., Poppe, D., Rupp, L., Schaub, A.,
687 and Wahner, A.: Product study of the reaction of OH radicals with isoprene in the
688 atmosphere simulation chamber SAPHIR, *J. Atmos. Chem.*, 55, 167–187, doi:
689 10.1007/s10874-006-9034-x, 2006.
- 690 Kato, S, Sato, T., Kaji, Y.: A method to estimate the contribution of unidentified VOCs
691 to OH reactivity. *Atmos. Environ.*, 45, 5531-5539, doi: 10.1016/j.atmosenv.2011.05.
692 074. 2011.
- 693 Kleinman, L. I., Daum, P. H., Imre, D. G., Lee. J. H., Lee. Y. N., Nunnermacker, L. J.,
694 Springston, S. R., Weinstein-Lloyd, J., Newman, L.: Ozone production in the New
695 York City urban plume. *J. Geophy. Res.-Atmos.*, 105, D11, 14495-14511, doi:
696 10.1029/2000 jd900011, 2000.
- 697 Kleinman, L. I.: Ozone production efficiency in an urban area, *J. Geophy. Res. –
698 atmos.*, 107, D23, 4733, doi: 10.1029/2002jd002529, 2002.
- 699 Kovacs, T. A., and Brune, W. H.: Total OH loss rate measurement, *J. Atmos. Chem.*,
700 39, 105-122, doi: 10.1023/a:1010614113786, 2001.
- 701 Kovacs, T. A., Brune, W. H., Harder, H., Martinez, M., Simpas, J. B., Frost, G. J.,
702 Williams, A. G., Jobson, B. T., Stroud, C., Young, V., Fried, A., and B., W.: Direct
703 measurements of urban OH reactivity during Nashville SOS in summer 1999, *J.
704 Environ. Monit.*, 5, 68-74, doi: 10.1039/b204339d, 2003.
- 705 Kumar V., Sinha, V.: VOC-OHM: a new technique for rapid measurements of ambient
706 total OH reactivity and volatile organic compounds using a single proton transfer
707 reaction mass spectrometer. *Int. J. of Mass Spectrom.*, 374, 55-63. 2014.
- 708 LaFranchi, B. W., Goldstein, A. H., and Cohen, R. C.: Observations of the
709 temperature dependent response of ozone to NO_x reductions in the Sacramento, CA

- 710 urban plume, *Atmos. Chem. Phys.*, 11, 6945-6960, doi: 10.5194/acp-11-6945-2011,
711 2011.
- 712 Lee, J. D., Young, J. C., Read, K. A., Hamilton, J. F., Hopkins, J. R., Lewis, A. C.,
713 Bandy, B. J., Davey, J., Edwards, P. M., Ingham, T., Self, D. E., Smith, S. C., Pilling,
714 M. J., and Heard, D. E.: Measurement and calculation of OH reactivity at a United
715 Kingdom coastal site, *J. Atmos. Chem.*, 64, 53-76, doi: 10.1007/s10874-010-9171-0,
716 2010.
- 717 Lei, W., Zavala, M., Foy, B. de., Volkamer, R., Molina, L. T.: Characterizing ozone
718 production and response under different meteorological conditions in Mexico City.
719 *Atmos. Chem. Phys.*, 8, 7571-7581, doi: 10.5194/acp-8-7571-2008, 2008.
- 720 Li, M., Shao, M., Li, L.-Y., Lu, S.-H., Chen, W.-T., and Wang, C.: Quantifying the
721 ambient formaldehyde sources utilizing tracers, *Chinese. Chem. Lett.*, 25, 1489-1491,
722 doi: 10.1016/j.cclet.2014.07.001, 2014.
- 723 Li, X., Brauers, T., Hofzumahaus, A., Lu, K., Li, Y. P., Shao, M., Wagner, T., and
724 Wahner, A.: MAX-DOAS measurements of NO₂, HCHO and CHOCHO at a rural site
725 in Southern China, *Atmos. Chem. Phys.*, 13, 2133-2151, doi:
726 10.5194/acp-13-2133-2013, 2013.
- 727 Liu, Y., Shao, M., Fu, L., Lu, S., Zeng, L., and Tang, D.: Source profiles of volatile
728 organic compounds (VOCs) measured in China: Part I, *Atmos. Environ.*, 42,
729 6247-6260, doi: 10.1016/j.atmosenv.2008.01.070, 2008.
- 730 Liu, Y., Shao, M., Kuster, W. C., Goldan, P. D., Li, X. H., Lu, S. H., de Gouw, J. A.:
731 Source identification of reactive hydrocarbons and oxygenated VOCs in the
732 summertime in Beijing. *Environ. Sci. Technol.*, 43, 75-81, doi: 10.1021/es801716n,
733 2009.
- 734 Liu, Y. H., Lu, K. D., Dong, H. B., Li, X., Cheng, P., Zou, Q., Wu, Y. S., Liu, X. G.,
735 Zhang, Y. H. In situ monitoring of atmospheric nitrous acid based on multi-pumping
736 flow system and liquid waveguide capillary cell. *J. Envion. Sci.* Accepted. 2016.
- 737 Liu, Z., Wang, Y., Vrekoussis, M., Richter, A., Wittrock, F., Burrows, J. P., Shao, M.,
738 Chang, C.-C., Liu, S.-C., Wang, H., and Chen, C.: Exploring the missing source of
739 glyoxal (CHOCHO) over China, *Geophy. Res. Lett.*, 39, L10812, doi:
740 10.1029/2012gl051645, 2012.
- 741 Lou, S., Holland, F., Rohrer, F., Lu, K., Bohn, B., Brauers, T., Chang, C. C., Fuchs, H.,
742 Häseler, R., Kita, K., Kondo, Y., Li, X., Shao, M., Zeng, L., Wahner, A., Zhang, Y.,
743 Wang, W., and Hofzumahaus, A.: Atmospheric OH reactivities in the Pearl River

- 744 Delta – China in summer 2006: measurement and model results, *Atmos. Chem. Phys.*,
745 10, 11243-11260, doi: 10.5194/acp-10-11243-2010, 2010.
- 746 Lu, K. D., Zhang, Y. H., Su, H., Brauers, T., Chou, C. C., Hofzumahaus, A., Liu, S. C.,
747 Kita, K., Kondo, Y., Shao, M., Wahner, A., Wang, J. L., Wang, X., and T., Z.: Oxidant
748 ($O_3 + NO_2$) production processes and formation regimes in Beijing, *J. Geophys.*
749 *Res.-Atmos.*, 115, D07303, doi: 10.1029/2009jd012714, 2010.
- 750 Lu, K. D., Hofzumahaus, A., Holland, F., Bohn, B., Brauers, T., Fuchs, H., Hu, M.,
751 Häseler, R., Kita, K., Kondo, Y., Li, X., Lou, S. R., Oebel, A., Shao, M., Zeng, L. M.,
752 Wahner, A., Zhu, T., Zhang, Y. H., and Rohrer, F.: Missing OH source in a suburban
753 environment near Beijing: observed and modelled OH and HO₂ concentrations in
754 summer 2006, *Atmos. Chem. Phys.*, 13, 1057-1080, doi: 10.5194/acp-13-1057-2013,
755 2013.
- 756 Mao, J. Q., Ren, X. R., Chen, S., Brune, W. H., Chen, Z., Martinez, M., Harder, H.,
757 Lefer, B., Rappengluck, B., Flynn, J., and M., L.: Atmospheric oxidation capacity in
758 the summer of Houston 2006: Comparison with summer measurements in other
759 metropolitan studies, *Atmos. Environ.*, 44, 4107-4115, doi: 10.1016/j.atmosenv.2009.
760 01.013, 2010.
- 761 Michoud, V., Hansen, R. F., Locoge, N., Stevens, P. S., and Dusanter, S.: Detailed
762 characterizations of the new Mines Douai comparative reactivity method instrument
763 via laboratory experiments and modeling, *Atmos. Meas. Tech.*, 8, 3537-3553, doi:
764 10.5194/amt-8-3537-2015, 2015.
- 765 Nölscher, A. C., Williams, J., Sinha, V., Custer, T., Song, W., Johnson, A. M., Axinte,
766 R., Bozem, H., Fischer, H., Pouvesle, N., Phillips, G., Crowley, J. N., Rantala, P.,
767 Rinne, J., Kulmala, M., Gonzales, D., Valverde-Canossa, J., Vogel, A., Hoffmann, T.,
768 Ouwersloot, H. G., Vilà-Guerau de Arellano, J., and Lelieveld, J.: Summertime total
769 OH reactivity measurements from boreal forest during HUMPPA-COPEC 2010,
770 *Atmos. Chem. Phys.*, 12, 8257-8270, doi: 10.5194/acp-12-8257-2012, 2012.
- 771 Nölscher, A. C., Yanez-Serrano, A. M., Wolff, S., de Araujo, A. C., Lavric, J. V.,
772 Kesselmeier, J., and Williams, J.: Unexpected seasonality in quantity and composition
773 of Amazon rainforest air reactivity, *Nature communications*, 7, 10383-10394, doi:
774 10.1038/ncomms10383, 2016.
- 775 Nakashima, Y., Kamei, N., Kobayashi, S., and Y., K.: Total OH reactivity and VOC
776 analyses for gasoline vehicular exhaust with a chassis dynamometer, *Atmos. Environ.*,
777 44, 468-475, doi: 10.1016/j.atmosenv.2009.11.006, 2010.

- 778 Pöschl, U., von Kuhlmann, R., Poisson, N., and Crutzen, P. J.: Development and
779 intercomparison of condensed isoprene oxidation mechanisms for global atmospheric
780 modeling, *J. Atmos. Chem.*, 37, 29–52, doi: 10.1023/A:1006391009798, 2000.
- 781 Ren, X. R., Harder, H., Martinez, M., Lesher, R. L., Olinger, A., Shirley, T., Adams, J.,
782 Simpas, J. B., and H., B. W.: HO_x concentrations and OH reactivity observations in
783 New York City during PMTACS-NY2001, *Atmos. Environ.*, 37, 3627-3637, doi:
784 10.1016/s1352-2310(03)00460-6, 2003.
- 785 Ren, X. R., Brune, W. H., Cantrell, C., Edwards, G. D., Shirley, T., Metcalf, A. R., and
786 L., L. R.: Hydroxyl and Peroxy Radical Chemistry in a Rural Area of Central
787 Pennsylvania: Observations and Model Comparisons, *J. Atmos. Chem.*, 52, 231-257,
788 doi: 10.1007/s10874-005-3651-7, 2005.
- 789 Ren, X. R., Brune, W. H., Mao, J. Q., Mitchell, M. J., Lesher, R. L., Simpas, J. B.,
790 Metcalf, A. R., Schwab, J. J., Cai, C., and Y., L.: Behavior of OH and HO₂ in the
791 winter atmosphere in New York City, *Atmos. Environ.* 40, 252-263, doi:
792 10.1016/j.atmosenv.2005.11.073, 2006a.
- 793 Ren, X. R., Brune, W. H., Olinger, A., Metcalf, A. R., Simpas, J. B., Shirley, T.,
794 Schwab, J. J., Bai, C., Roychowdhury, U., Li, Y., Cai, C., Demerjian, K. L., He, Y.,
795 Zhou, X. H., Gao, H., and J., H.: OH, HO₂, and OH reactivity during the
796 PMTACS–NY Whiteface Mountain 2002 campaign: Observations and model
797 comparison, *J. Geophys. Res.-Atmos.*, 111, doi: 10.1029/2005jd006126, 2006b.
- 798 Sadanaga, Y., Yoshino, A., Kato, S., Yoshioka, A., Watanabe, K., Miyakawa, T.,
799 Hayashi, I., Ichikawa, M., Matsumoto, J., Nishiyama, A., Akiyama, N., Kanaya, Y.,
800 and Y., K.: The importance of NO₂ and volatile organic compounds in the urban air
801 from the viewpoint of the OH reactivity, *Geophy. Res. Lett.*, 31, L08102, doi:
802 10.1029/2004gl019661, 2004.
- 803 Sadanaga, Y., Yoshino, A., Kato, S., and Y., K.: measurements of OH reactivity and
804 photochemical ozone production in the urban atmosphere, *Environ. Sci. Technol.*, 39,
805 8847-8852, doi: 10.1021/es049457p, 2005.
- 806 Sheehy, P. M., Volkamer, R., Molina, L. T., and Molina, M. J.: Oxidative capacity of
807 the Mexico City atmosphere – Part 2: A RO_x radical cycling perspective, *Atmos.*
808 *Chem. Phys.*, 10, 6993-7008, doi: 10.5194/acp-10-6993-2010, 2010.
- 809 Shirley, T. R., Brune, W. H., Ren, X. R., Mao, J. Q., Lesher, R., Cardenas, B.,
810 Volkamer, R., Molina, L. T., Molina, M. J., Lamb, B., Velasco, E., Jobson, T., and M.,
811 A.: Atmospheric oxidation in the MCMA during April 2003, *Atmos. Chem. Phys.*, 6,

- 812 2753-2765, doi: 10.5194/acp-6-2753-2006, 2006.
- 813 Sinha, V., Williams, J., Crowley, J. N., and J., L.: The Comparative Reactivity Method
814 - a new tool to measure total OH reactivity in ambient air, *Atmos. Chem. Phys.*, 8,
815 2213-2227, doi: 10.5194/acp-8-2213-2008, 2008.
- 816 Sinha, V., Custer, T. G., Kluepfel, T., and Williams, J.: The effect of relative humidity
817 on the detection of pyrrole by PTR-MS for OH reactivity measurements, *Int. J. Mass*
818 *Spectrom.*, 282, 108-111, doi: 10.1016/j.ijms.2009.02.019, 2009.
- 819 Sinha, V., Williams, J., Lelieveld, J., Ruuskanen, T. M., Kalos, M. K., Patokoski, L.,
820 Hellen, H., Hakola, H., Mogensen, D., Boy, M., Rinne, L., and M., K.: OH reactivity
821 measurements within a boreal forest - evidence for unknown reactive emissions,
822 *Environ. Sci. Technol.*, 44, 6614-6620, doi: 10.1021/es101780b, 2010.
- 823 Sinha, V., Williams, J., Diesch, J. M., Drewnick, F., Martinez, M., Harder, H., Regelin,
824 E., Kubistin, D., Bozem, H., Hosaynali-Beygi, Z., Fischer, H., Andrés-Hernández, M.
825 D., Kartal, D., Adame, J. A., and Lelieveld, J.: Constraints on instantaneous ozone
826 production rates and regimes during DOMINO derived using in-situ OH reactivity
827 measurements, *Atmos. Chem. Phys.*, 12, 7269-7283, doi: 10.5194/acp-12-7269-2012,
828 2012.
- 829 Stockwell, W. R., Kirchner, F., Kuhn, M., and Seefeld, S.: A new mechanism for
830 regional atmospheric chemistry modeling, *J. Geophys. Res.-Atmos.*, 102, D22,
831 25847-25879, doi: 10.1029/97jd00849, 1997.
- 832 Stone, D., Whalley, L. K., and Heard, D. E.: Tropospheric OH and HO₂ radicals: field
833 measurements and model comparisons, *Chem. Soc. Rev.*, 41, 6348-6404, doi:
834 10.1039/c2cs35140d, 2012.
- 835 Tan, Z. F., Fuchs, H., Zhang, Y. H., et al., *Atmos. Chem. Phys.*, in preparation.
- 836 Wang, M., Zeng, L., Lu, S., Shao, M., Liu, X., Yu, X., Chen, W., Yuan, B., Zhang, Q.,
837 Hu, M., and Zhang, Z.: Development and validation of a cryogen-free automatic gas
838 chromatograph system (GC-MS/FID) for online measurements of volatile organic
839 compounds, *Anal. Methods*, 6, 9424-9434, doi: 10.1039/c4ay01855a, 2014a.
- 840 Wang, M., Shao, M., Chen, W. T., Yuan, B., Lu, S. H., Zhang, Q., Zeng, L. M., Wang,
841 Q.: A temporally and spatially resolved validation of emission inventories by
842 measurements of ambient volatile organic compounds in Beijing, China. *Atmos.*
843 *Chem. Phys.* 14, 5871-5891, doi: 10.5194/acp-14-5871-2014, 2014b.
- 844 Wang, M., Shao, M., Chen, W., Lu, S., Liu, Y., Yuan, B., Zhang, Q., Zhang, Q., Chang,
845 C. C., Wang, B., Zeng, L., Hu, M., Yang, Y., and Li, Y.: Trends of non-methane

- 846 hydrocarbons (NMHC) emissions in Beijing during 2002–2013, *Atmos. Chem. Phys.*,
847 15, 1489-1502, doi: 10.5194/acp-15-1489-2015, 2015.
- 848 Wang, T., Ding, A., Gao, J., and Wu, W. S.: Strong ozone production in urban plumes
849 from Beijing, China. *Geophys. Res. Lett.*, 33, L21806, doi: 10.1029/2006gl027689,
850 2006.
- 851 Whalley, L. K., Stone, D., Bandy, B., Dunmore, R., Hamilton, J. F., Hopkins, J., Lee, J.
852 D., Lewis, A. C., and Heard, D. E.: Atmospheric OH reactivity in central London:
853 observations, model predictions and estimates of in situ ozone production, *Atmos.*
854 *Chem. Phys.*, 16, 2109-2122, doi: 10.5194/acp-16-2109-2016, 2016.
- 855 Williams, J.: Provoking the air, *Environ. Chem.*, 5, 317-319, doi:10.1071/en08048,
856 2008.
- 857 Williams, J., and Brune, W. H.: A roadmap for OH reactivity research, *Atmos.*
858 *Environ.*, 106, 371-372, doi: 10.1016/j.atmosenv.2015.02.017, 2015.
- 859 Williams, J., Keßel, S. U., Nölscher, A. C., Yang, Y. D., Lee, Y. N., Yáñez-Serrano, A.
860 M., Wolff, S., Kesselmeier, J., Klüpfel, T., Lelieveld, J., and Shao, M.: Opposite OH
861 reactivity and ozone cycles in the Amazon rainforest and megacity Beijing:
862 Subversion of biospheric oxidant control by anthropogenic emissions, *Atmos.*
863 *Environ.*, 125, 112-118, doi: 10.1016/j.atmosenv.2015.11.007, 2016.
- 864 Wu, Y., Yang, Y. D., Shao, M., and Lu, S. H.: Missing in total OH reactivity of VOCs
865 from gasoline evaporation, *Chinese. Chem. Lett.*, 26, 1246-1248, doi:
866 10.1016/j.cclet.2015.05.047, 2015.
- 867 Yang, Y., Shao, M., Wang, X., Nölscher, A. C., Kessel, S., Guenther, A., and Williams,
868 J.: Towards a quantitative understanding of total OH reactivity: A review, *Atmos.*
869 *Environ.*, 134, 147-161, doi: 10.1016/j.atmosenv.2016.03.010, 2016.
- 870 Yoshino, A., Sadanaga, Y., Watanabe, K., Kato, S., Miyakawa, Y., Matsumoto, J., and
871 Y., K.: Measurement of total OH reactivity by laser-induced pump and probe
872 technique—comprehensive observations in the urban atmosphere of Tokyo, *Atmos.*
873 *Environ.*, 40, 7869-7881, doi: 10.1016/j.atmosenv.2006.07.023, 2006.
- 874 Yoshino, A., Nakashima, Y., Miyazaki, K., Kato, S., Suthawaree, J., Shimo, N.,
875 Matsunaga, S., Chatani, S., Apel, E., Greenberg, J., Guenther, A., Ueno, H., Sasaki, H.,
876 Hoshi, J., Yokota, H., Ishii, K., and Kajii, Y.: Air quality diagnosis from
877 comprehensive observations of total OH reactivity and reactive trace species in urban
878 central Tokyo, *Atmos. Environ.*, 49, 51-59, doi: 10.1016/j.atmosenv.2011.12.029,
879 2012.

- 880 Yuan, B., Shao, M., de Gouw, J., Parrish, D. D., Lu, S., Wang, M., Zeng, L., Zhang,
881 Q., Song, Y., Zhang, J., and Hu, M.: Volatile organic compounds (VOCs) in urban air:
882 How chemistry affects the interpretation of positive matrix factorization (PMF)
883 analysis, *J. Geophys. Res.-Atmos.*, 117, D24302, doi: 10.1029/2012jd018236, 2012.
- 884 Zhang, Q., Yuan, B., Shao, M., Wang, X., Lu, S., Lu, K., Wang, M., Chen, L., Chang,
885 C. C., and Liu, S. C.: Variations of ground-level O₃ and its precursors in Beijing in
886 summertime between 2005 and 2011, *Atmos. Chem. Phys.*, 14, 6089-6101, doi:
887 10.5194/acp-14-6089-2014, 2014.
- 888 Zhang, Y. H., Su, H., Zhong, L. J., Cheng, Y. F., Zeng, L. M., Wang, X. S., Xiang, Y.
889 R., Wang, J. L., Gao, D. F., and Shao, M.: Regional ozone pollution and
890 observation-based approach for analyzing ozone–precursor relationship during the
891 PRIDE-PRD2004 campaign, *Atmos. Environ.*, 42, 6203-6218, doi:
892 10.1016/j.atmosenv.2008.05.002, 2008.
- 893 Zhao, C., Wang, Y. H., Zeng, T.,: East China Plains: a "Basin" of ozone pollution,
894 *Environ. Sci. Technol.*, 43, 1911-1915, doi: 10.1021/es8027764, 2009.
- 895 Zheng, J. Y., Shao, M., Che, W. W., Zhang, L. J., Zhong, L. J., Zhang, Y. H., Streets,
896 D., Speciated VOC emission inventory and spatial patterns of ozone formation
897 potential in the Pearl River Delta, China. *Environ. Sci. Technol.* 43, 8580–8586, doi:
898 10.1021/es901688e, 2009.
- 899 Zheng, J. Y., Zhong, L. J., Wang, T., Louie, P. K. K., Li, Z. C.: Ground-level ozone in
900 the Pearl River Delta region: analysis of data from a recently established regional air
901 quality monitoring network. *Atmos. Environ.* 44, 814-823, doi: 10.1016/j.atmosenv.
902 2009.11.032, 2010.
- 903 Zhao, W., Cohan, D. S., Henderson, B. H.: Slower ozone production in Houston,
904 Texas following emission reductions: evidence from Texas Air Quality Studies in
905 2000 and 2006. *Atmos. Chem. Phys.* 14, 2777-2788, doi: 10.5194/acp-14-2777-2014,
906 2014.
- 907
- 908
- 909
- 910
- 911
- 912

Table 1 Total OH reactivity measurements in urban areas

Campaign	Site	Year	method	$k_{OH}(\text{measured}, \text{s}^{-1})^a$	$k_{OH}(\text{calculated}, \text{s}^{-1} \text{ if it is a value})^b$	Measured species ^c	Reference
SOS	Nashville, US	summer, 1999	LIF-flow tube	11.3	7.2	SFO	Kovacs et al., 2001; 2003;
PMTACS-NY 2001	NY, US	summer, 2001	LIF-flow tube	15~25	within 10%	SFO	Ren et al., 2003
PMTACS-NY 2004	NY, US	winter, 2004	LIF-flow tube	18-35	statistically lower	SF	Ren et al., 2006a
MCMA-2003	Mexico City, Mexico	spring, 2003	LIF-flow tube	10~120	30% less than	- ^d	Shirley et al., 2006
TexAQS	Houston, US	summer, 2000	LIF-flow tube	7~12	agree well	SFO	Mao et al., 2010
TRAMP2006	Houston, US	summer, 2006	LIF-flow tube	9-22	agree well	SFOB	Mao et al., 2010
Tokyo, Japan	2003-2004	LP-LIF	10~100	30% less than	SFOB	Sadanaga et al., 2004; Yoshino et al., 2006	
Tokyo, Japan	summer, 2006	LP-LIF	10~55	30% less than	SFOB	Chatani et al., 2009	
Tokyo, Japan	spring, 2009	LP-LIF	10~35	22% less than	SFOB	Kato et al., 2011	
Tokyo, Japan	winter, 2007, autumn, 2009	LP-LIF	10~80	10~15 less than	SFOB	Yoshino et al., 2012	

Table 1 Total OH reactivity measurements in urban areas (continued)

	Mainz, German	summer, 2005	CRM	10.4		-	Sinha et al., 2008
MEGAPOLI	Paris, France	winter, 2010	CRM	10~130	10~54% less than	SO	Dolgorouky et al., 2012
ClearfLo	London, England	summer, 2012	LP-LIF	10-116	20~40%	SFOB	Whalley et al., 2016
	Lille, France	autumn , 2012	CRM, LP-LIF	~70	Reasonable agreement	SFO	Hansen et al., 2015
	Dunkirk, France	summer, 2014	CRM	10-130		-	Michoud et al., 2015

914 a. For sources from different studies, the measured reactivity was presented as the averaged results, or ranges of diurnal variations, or the ranges of the whole
915 campaign.

916 b. For sources of different studies, the calculated reactivity was presented within an uncertainty range, as a percentage reduction or s^{-1} reduction.

917 c. Measured species that have been used for the calculated reactivity (following Lou et al., 2010): S = inorganic compounds (CO, NO_x, SO₂ etc) plus hydrocarbons
918 (including isoprene); F = formaldehyde; O = OVOCs other than formaldehyde; B = BVOCs other than isoprene;

919 d. “_” means a lack of information regarding what has been measured or how long it has been measured.

920

921

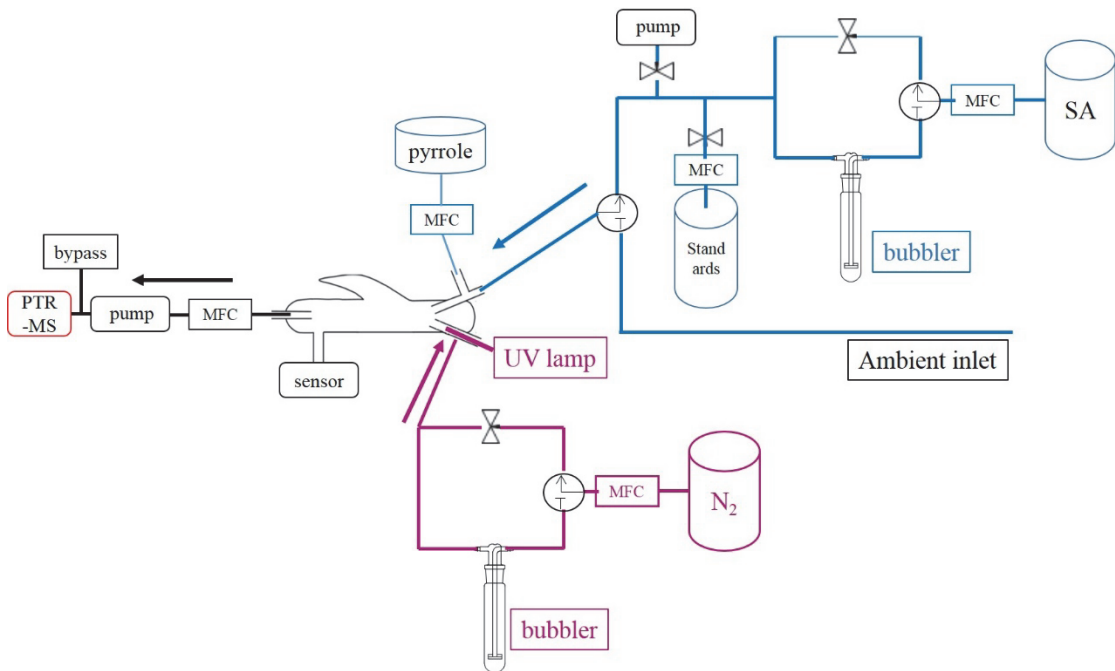
922

923

924

Table2 Total OH reactivity measurements in suburban and surrounding areas

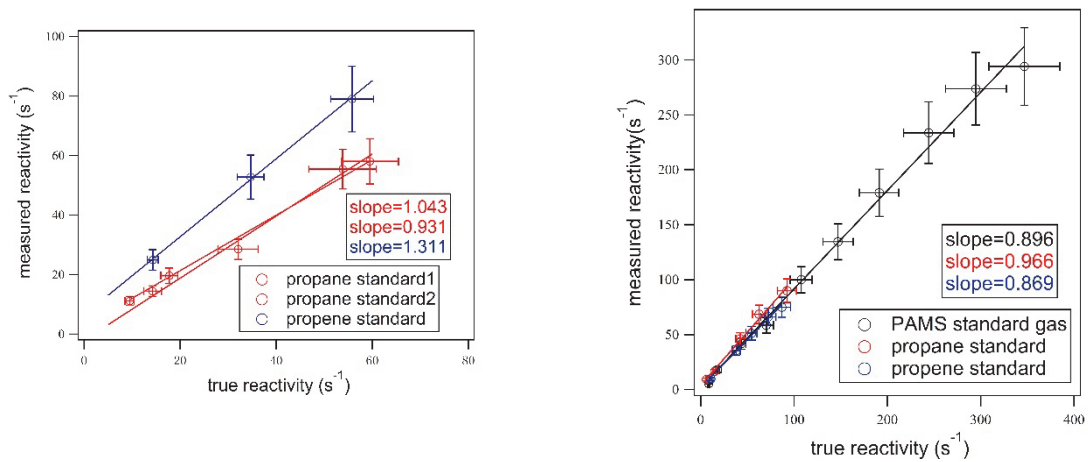
Campaign	Site	Year	method	$k_{OH(measured)}$ (s^{-1})	$k_{OH(calculated)}$ (s^{-1} if it is a value)	Measured Species	Reference
PMTACS-NY2002	Central Pennsylvania, US Whiteface Mountain, US	spring, 2002 summer, 2002	LIF-flow tube LIF-flow tube	6.1 5.6	within 10%	-	Ren et al., 2005
TORCH-2	Weybourne, England	spring, 2004	LIF-flow tube	4.85	2.95	SFO	Ren et al., 2006b
CareBeijing-2006	Yufa, China	summer, 2006	LP-LIF	10-30	agree well	S	Ingham et al., 2009
PRIDE-PRD	Backgarden, China	summer, 2006	LP-LIF	10~120	50% less than	S	Lee et al., 2010; Lu et al., 2010; 2013
DOMINO	El Arenosillo, Spain	winter, 2008	CRM	6.3~85		SF	Sinha et al., 2012
		spring, 2013	CRM	53	23	SFOB	Kumar & Sinha., 2014



927

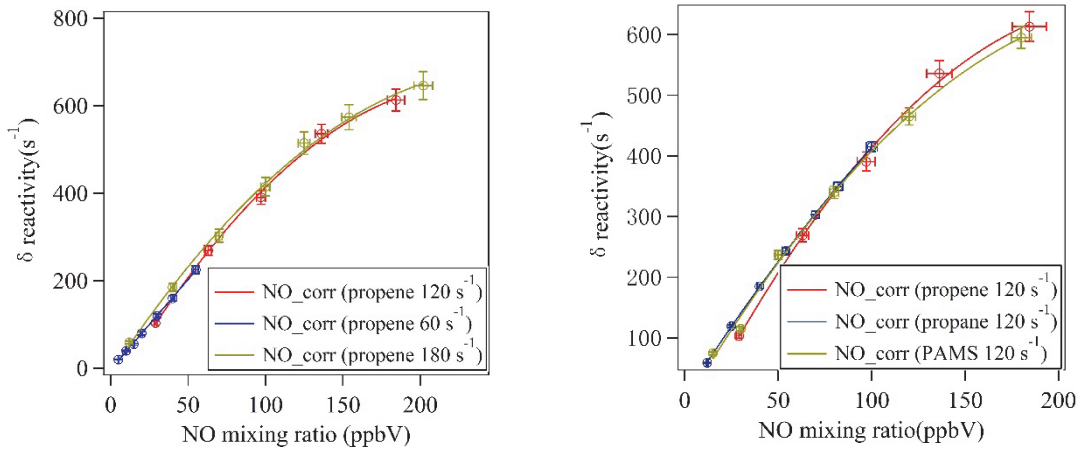
928 Fig 1 Schematic figures of CRM system in Beijing and Heshan observations.

929 Blue color represents ambient air or synthetic air injection system, purple color
 930 represents OH generating system, black color represents the detection system.
 931 Pressure is measured by the sensor connected to the glass reaction.



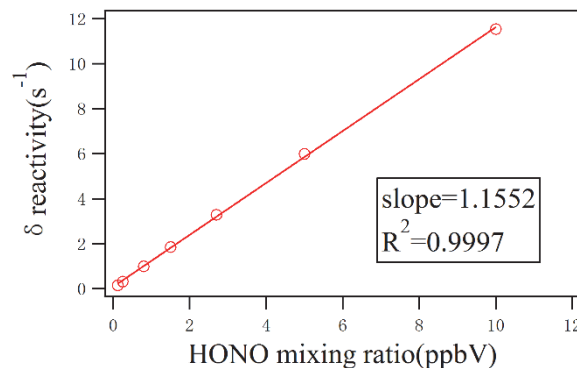
932 Fig 2 OH reactivity calibration in Beijing (left) and Heshan (right).

933 Left: Calibration in Beijing used two single standards: propane, propene;
 934 Right: Calibration in Heshan used three standards: propane, propene, mixed PAMS 56
 935 NMHCs.
 936 Error bars stand for estimated uncertainty on the measured and true reactivity.



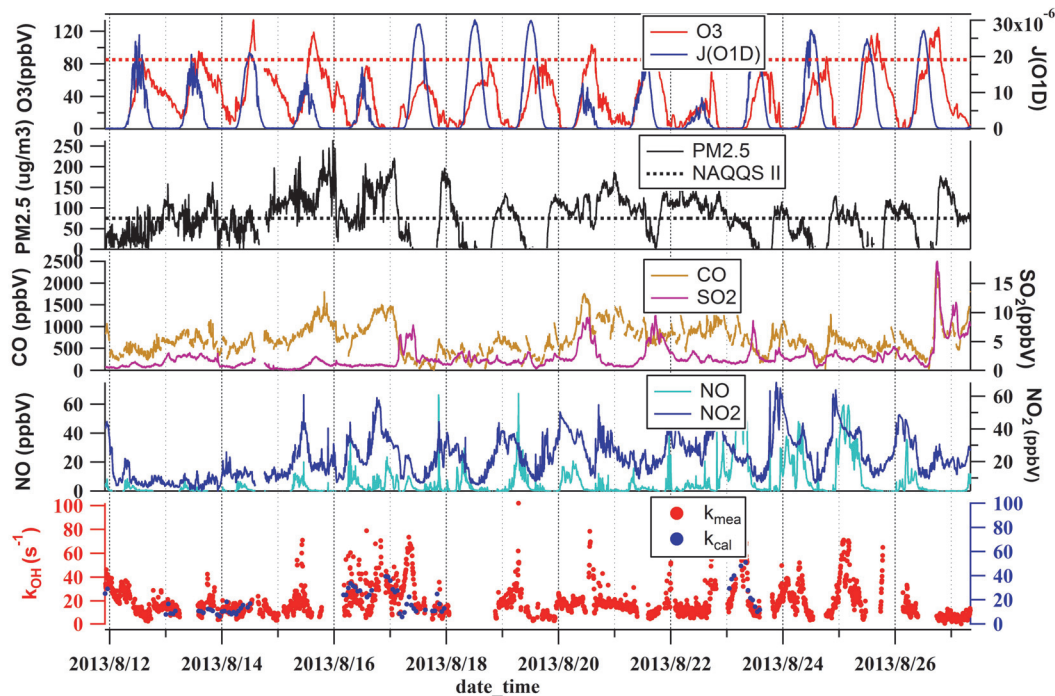
937

938 Fig 3 NO-correction experiments and fitting curves in Heshan 2014.
 939 Left: NO-correction experiments with different mixing ratios of propene standard gas;
 940 Right: NO-correction experiments with different standard gases at the same reactivity
 941 level: 120 s^{-1} .
 942 Error bars stand for estimated uncertainty on the NO mixing ratios and difference in
 943 reactivity.



944

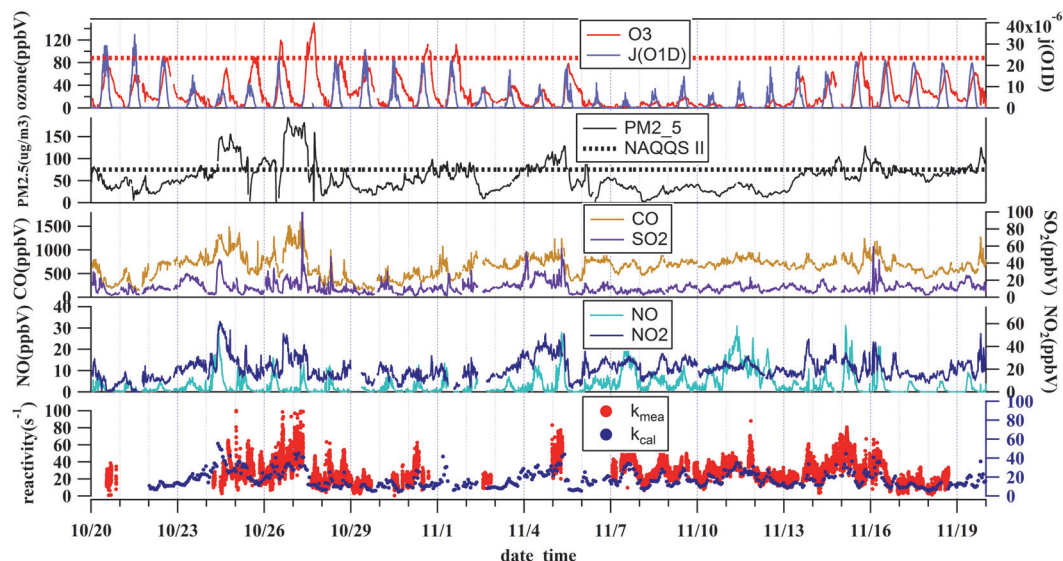
945 Fig 4 HONO-correction experiments and the fitting curve in Heshan 2014.
 946
 947



948 Fig 5-a Time series of meteorological parameters and inorganic trace gases during
949 August 2013 in Beijing.

950 Red and black dashed lines are Grade II of National Ambient Air Quality Standard.

951

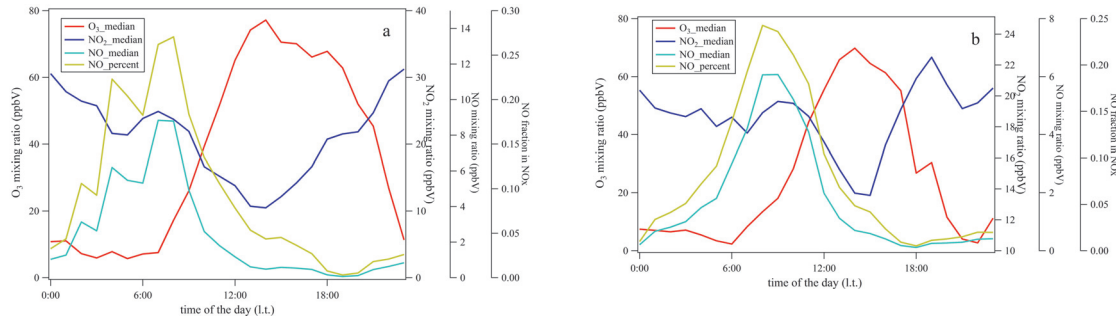


952 Fig 5-b Time series of meteorological parameters and inorganic trace gases during
953 October-November, 2014 in Heshan.

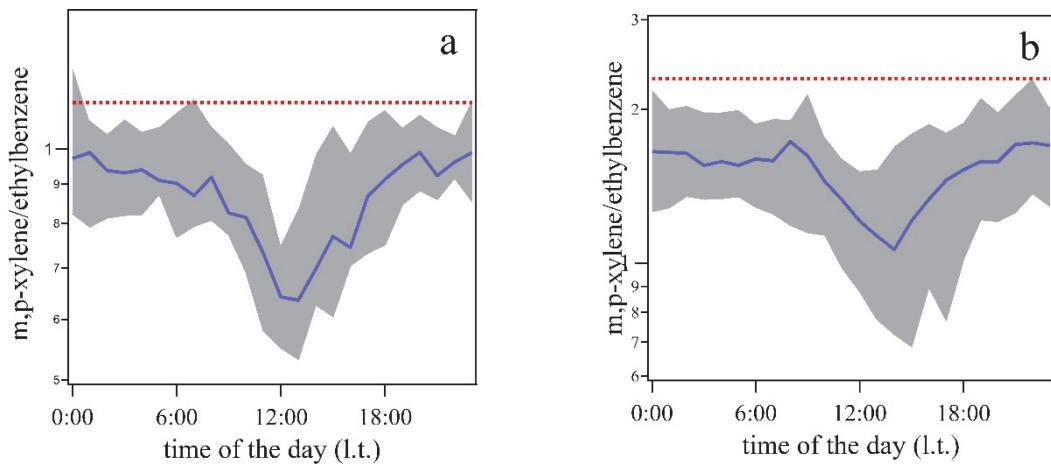
954 Red and black dashed lines are Grade II of National Ambient Air Quality Standard.

955

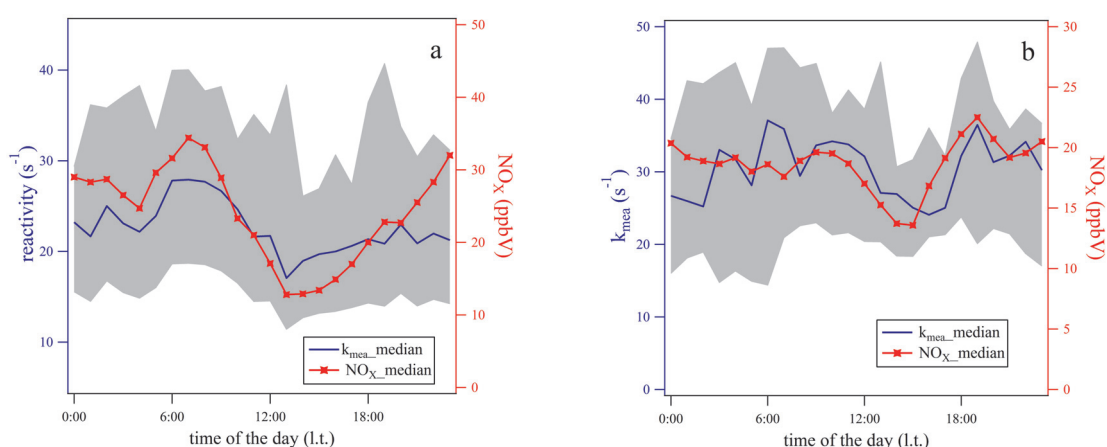
956



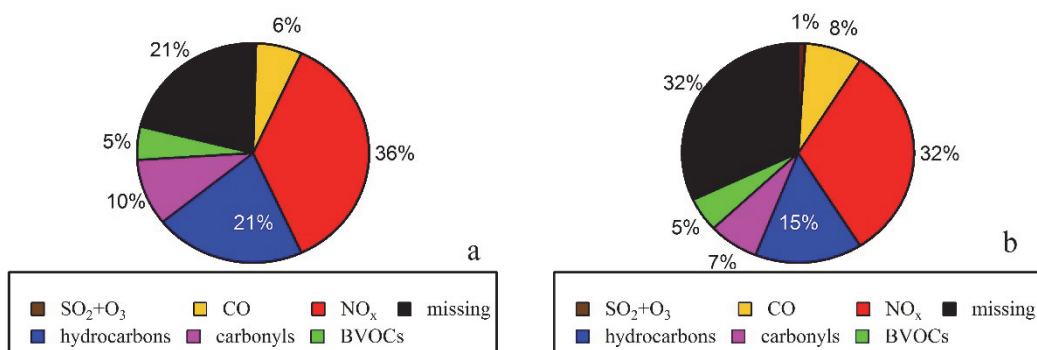
957 Fig 6 Diurnal variations of O_3 , NO , NO_2 and relative contribution of NO to NO_x
958 in Beijing 2013 (a) and Heshan 2014 (b)
959



960
961 Fig 7 Ratios of m,p-xylene to ethylbenzene in Beijing 2013 (a) and Heshan 2014 (b)
962 Red dots line: the highest m,p-xylene to ethylbenzene ratio, assumed as emission
963 ratios of m,p-xylene to ethylbenzene, 1.15 ppbV ppbV⁻¹ in Beijing 2013 (a) and 2.3
964 ppbV ppbV⁻¹ in Heshan 2014 (b).
965 Shaded regions: Standard deviation for the ratios during the campaign average.
966

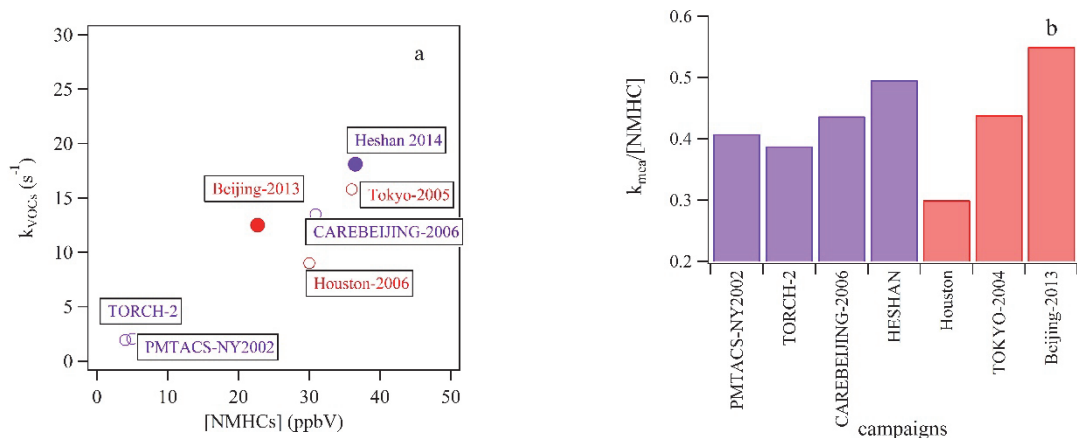


967
968 Fig 8 Diurnal variation of hourly median results of measured OH reactivity and NO_x
969 mixing ratios in Beijing (a) and Heshan (b)



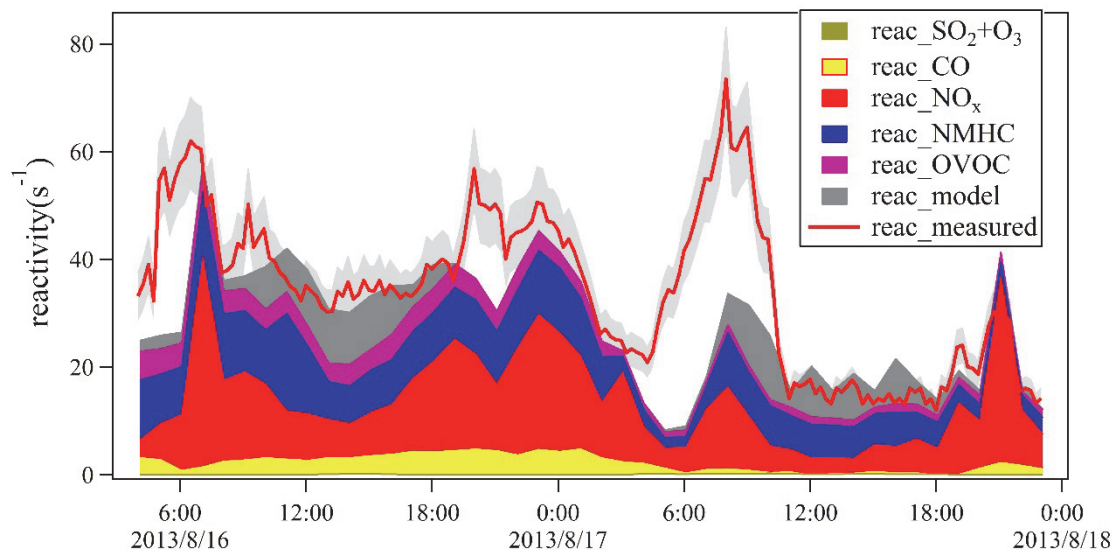
971 Fig 9 Composition of measured reactivity in Beijing (a) and Heshan (b)

972

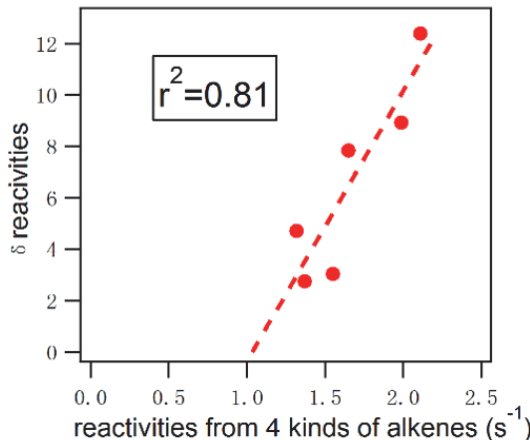


973

974 Fig 10 a: Comparison of VOCs reactivity and measured NMHCs in urban and
975 suburban observations.976 b: Comparison of the ratio between VOCs reactivity and measured NMHCs in urban
977 and suburban observations



978



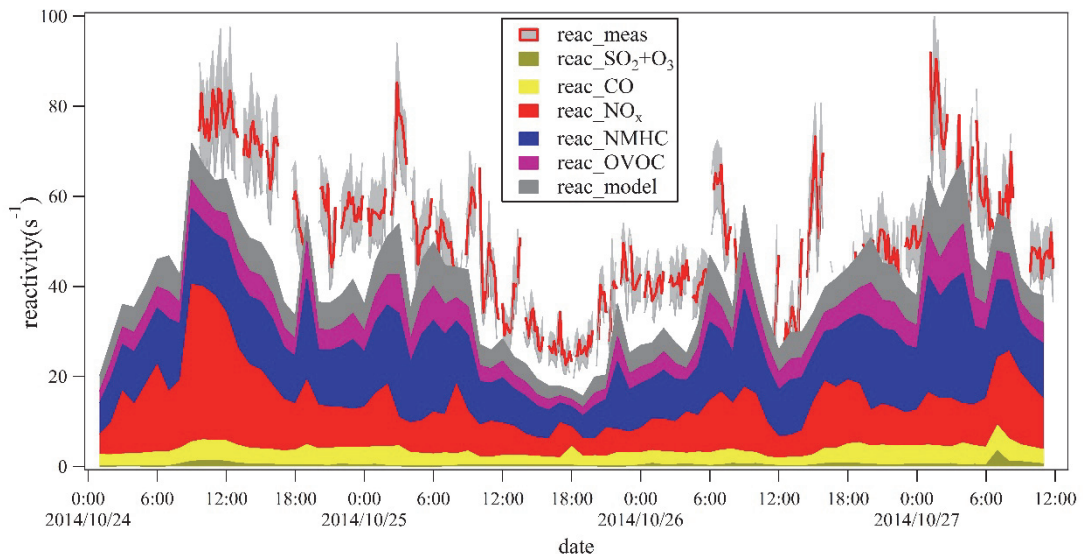
979

980 Fig 11 Upper panel: Comparison between measured and calculated reactivity in
981 Beijing August 16th to 18th 2013.

982 Shallow shaded region: uncertainty of measured reactivity. The same shallow shaded
983 region in Fig 12 represents the same.

984 Lower panel: Correlation between missing reactivity measured in 2013 and reactivity
985 assumed from branched-chain alkenes from 2005 in diurnal patterns. The 4
986 branched-alkenes are iso-butene, 2-methyl-1-butene, 3-methyl-1-butene and
987 2-methyl-2-butene.

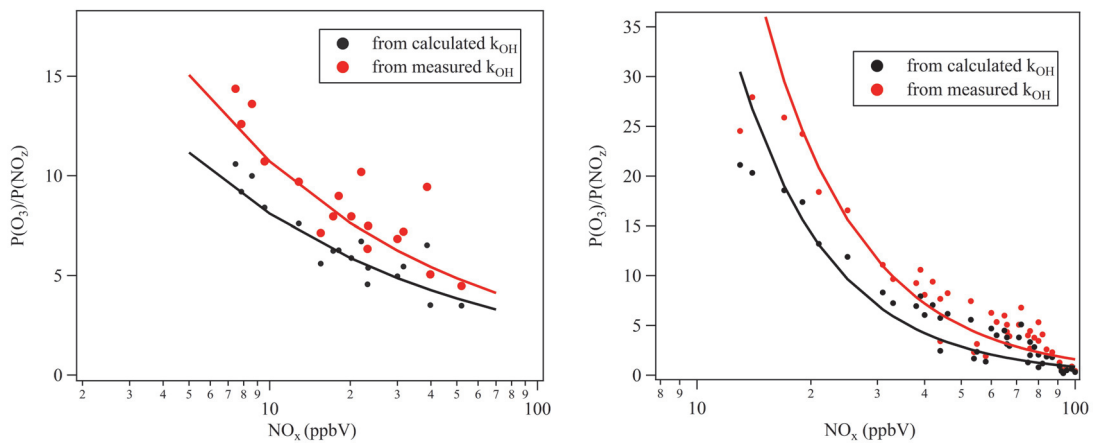
988



990 Fig 12 Comparison between measured reactivity and calculated reactivity as well as
 991 modelled reactivity in Heshan between October 24th and 27th 2014.

992

993



994

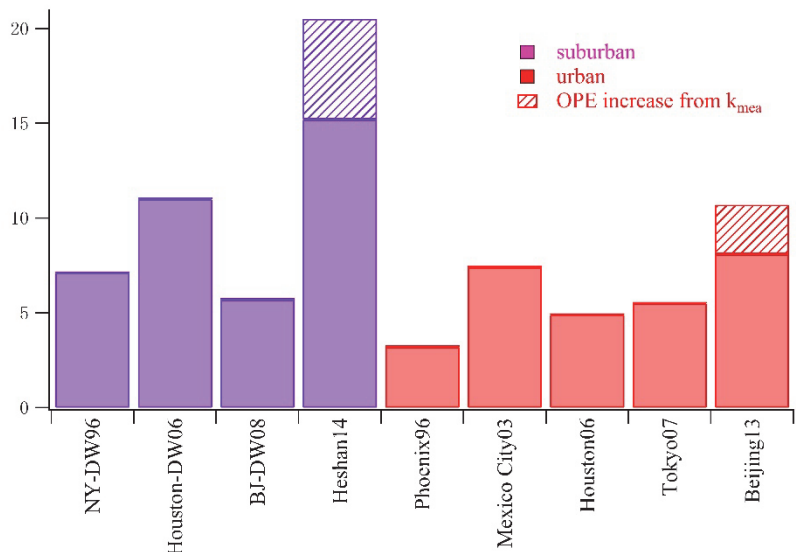
995

a

b

996 Fig 13 Comparison between OPE calculated from measured reactivity and calculated
 997 reactivity in Beijing (a) and Heshan (b).

998



999

1000 Fig 14 Comparison between the OPE results in this study and other results from
 1001 literatures. The comparison is made with the $NO_x = 20$ ppbV. “DW” is in abbreviation
 1002 of downwind.

1003